Talanta 119 (2014) 452–457

Contents lists available at ScienceDirect

Talanta

journal homepage: www.elsevier.com/locate/talanta

Highly selective enrichment of phosphopeptides with high-index facets exposed octahedral tin dioxide nanoparticles for mass spectrometric analysis

Rongna Ma [a], Junjie Hu [a], Zongwei Cai [b], Huangxian Ju [a,*]

[a] State Key Laboratory of Analytical Chemistry for Life Science, School of Chemistry and Chemical Engineering, Nanjing University, Nanjing 210093, PR China
[b] Department of Chemistry, Hong Kong Baptist University, Kowloon Tong, Kowloon, Hong Kong, PR China

ARTICLE INFO

Article history:
Received 21 September 2013
Received in revised form
14 November 2013
Accepted 16 November 2013
Available online 22 November 2013

Keywords:
Tin dioxide
Matrix-assisted laser desorption/ionization mass spectrometry
Phosphopeptide
Enrichment

ABSTRACT

High-index facets exposed octahedral tin dioxide (SnO_2) nanoparticles were successfully synthesized and applied to selectively enrich phosphopeptides for mass spectrometric analysis. The high selectivity and capacity of the octahedral SnO_2 nanoparticles were demonstrated by effectively enriching phosphopeptides from digests of phosphoprotein (α- or β-casein), protein mixtures of β-casein and bovine serum albumin, milk, and human serum samples. The unique octahedral SnO_2 with abundant unsaturated coordination Sn atoms exhibited enhanced affinity and selective coordination ability with phosphopeptides due to their high chemical activity. The strong affinity led to highly selective capture and enrichment of phosphopeptides for sensitive detection through the bidentate bonds formed between surface atoms and phosphate. The phosphopeptides could be detected in β-casein down to 4×10^{-9} M or in the mixture of β-casein and BSA with a molar ratio of even 1:100. The performance in selective enrichment of phosphopeptides from drinking milk and human serum showed powerful evidence of high selectivity and efficiency in identifying the low-abundant phosphopeptides from complicated biological samples. This work provided a way to improve the physical and chemical properties of materials by tailoring their exposed facets for selective enrichment of phosphopeptides.

1. Introduction

Protein phosphorylation, one of the most important protein post-translational modifications, plays the key roles in regulating complex biological processes, such as cellular growth, division, and signaling transduction. Thus, the identification and localization of phosphorylation sites in proteins are of important significance for understanding biochemical pathways and disease states [1–4]. Mass spectrometry (MS) has emerged as the most powerful technique for examining the phosphorylation process due to its ultrahigh sensitivity, wide dynamic range and superior speed in analyzing complex samples. Unfortunately, owing to the low abundance of phosphorylated peptides, the substoichiometry of phosphorylation and the signal suppression of non-phosphorylated peptides, phosphorylation analysis still remains a great challenge for comprehensive understanding of protein phosphorylation [5,6]. Therefore, selective capture and enrichment of phosphorylated peptides from the complex mixtures prior to the interrogation of phosphorylation by MS has become an interesting research topic in bioanalysis.

A variety of enrichment strategies such as immobilized metal ion affinity chromatography (IMAC) [7–11], immunoprecipitation [12,13], and metal oxide affinity chromatography (MOAC) [14–17] have been developed to selectively capture and enrich the targeted phosphopeptides. Although IMAC is the most widely used technology, MOAC has shown higher capacity for selective enrichment of phosphopeptides and phosphoproteins [18]. Recently, various metal oxides such as titanium dioxide (TiO_2) [19–21], zirconium dioxide [18], alumina [22], tin dioxide (SnO_2) [23–28] and some composites [29–32] have been demonstrated to be specific in the trapping of phosphoproteins/phosphopeptides due to their specific and reversible interaction with phosphate groups through Lewis acid–base and bidentate bonds [14]. Especially, SnO_2 has been identified as an affinity probe for phosphopeptide enrichment and shown more excellent selectivity and less nonspecific binding than TiO_2 [23].

As an affinity probe, SnO_2 has been used for preparation of gas sensors [33,34], photocatalysis [35] and fabrication of lithium rechargeable batteries [36]. Recently, some surface scientists have demonstrated that the performance of SnO_2 in gas sensing and catalysis is greatly affected by the surface structure. In principle, phosphopeptides enrichment by metal-oxide like SnO_2 occurring on the surface metal-oxide, considering the fact that high-energy

* Corresponding author. Tel/fax.: +86 25 83593593.
E-mail address: hxju@nju.edu.cn (H. Ju).

0039-9140/$ - see front matter © 2013 Elsevier B.V. All rights reserved.
http://dx.doi.org/10.1016/j.talanta.2013.11.049

or high-index facets with abundant unsaturated coordination atoms usually exhibit high surface activity [37–43], the morphological control of metal oxides may provide a way to further tailor the physical and chemical properties of nanomaterials. Thus it is possible to use high-index facets tin oxide nanoparticles for efficiently improving sensitivity and selectivity of phosphopeptides enrichment.

This work investigated the high-index facets of octahedral SnO_2 nanoparticles and observed the strong affinity of the nanoparticles to phosphopeptides due to the formation of bidentate bonds between high-density surface Sn atoms and phosphate [14]. The high surface activity made the nanoparticles become a novel metal oxide material for selective enrichment of phosphopeptides. By coupling with the enrichment process, a mass spectrometric method was thus proposed for simultaneous detection of three phosphopeptides in the tryptic digest of β-casein down to 4×10^{-9} M. The performance of octahedral SnO_2 nanoparticles in selective enrichment of low abundance phosphopeptides from the tryptic digests of drinking milk and human serum clearly demonstrated its great capability in phosphoproteome analysis for real biological samples. This is the first example using the high-index facets exposed metal oxide materials for phosphopeptide capture, and provides the promising application in proteomics.

2. Experimental

2.1. Materials and reagents

Tin (IV) chloride pentahydrate ($SnCl_4\cdot5\,H_2O$), trifluoroacetic acid (TFA, ≥90%), ammonium bicarbonate, DL-dithiothreitol (DTT), iodoacetamide (IAA), phosphoric acid (≥85%), β-casein (Mw ~24 kDa), bovine serum albumin (BSA, Mw ~66 kDa), α-casein (Mw ~24 kDa) and 2,5-dihydroxybenzoic acid (DHB) were purchased from Sigma-Aldrich (St. Louis, MO, USA). Sequencing grade modified trypsin was obtained from Promega (Madison, USA). Acetonitrile (ACN) was obtained from Merck (Darmstadt, Germany). Hydrochloric acid (36.0–38.0%), polyvinylpyrrolidone (PVP, K-30) and ethanol (≥99.7%) were purchased from Nanjing Chemical Reagent CO., Ltd. (China). All these reagents were used as received without further purification. Drinking milk was purchased from a local grocery store. The clinical serum samples were from Jiangsu Institute of Cancer Prevention and Cure. All aqueous solutions were prepared using ultra-pure water (≥18 MΩ, Milli-Q, Millipore).

2.2. Synthesis of octahedral tin dioxide nanoparticles

Octahedral tin dioxide nanoparticles with high-index {221} facets were synthesized through a hydrothermal route at 200 °C for 12 h according to previous report with some modifications [44]. About 1.2 mL of concentrated hydrochloric acid (mass fraction 36.5–38%) was added to 12 mL ethanol/distilled water (1/1, v/v) under intense ultrasonic treatment. About 0.5 g of $SnCl_4\cdot5\,H_2O$ was added into the mixture, sonicated for 15 min at a frequency of 40 kHz, and stirred for 60 min. Then 0.315 g PVP was added, sonicated for 15 min, and stirred for 60 min. The obtained solution was transferred to a Teflon-lined stainless steel autoclave and kept at 200 °C for 12 h. The product was further underwent centrifugation and washed with deionized water and ethanol several times, and then dried in air at 80 °C for 24 h.

2.3. Characterization of octahedral tin dioxide nanoparticles

Scanning electron microscopic images were obtained with a Hitachi S-3000 N scanning electron microscope at an acceleration voltage of 10 kV. The transmission electron microscopic (TEM) images were gained on a JEM-2100 TEM (JEOL, Japan). Powder X-ray diffraction patterns were recorded on Rigaku Dmax 2200 X-ray diffractometer with Cu Kα radiation ($\lambda=1.5416$ A).The dynamic light-scattering measurement was carried out using a Brookhaven BI-9000AT instrument (Brookhaven Instruments Corporation).

2.4. Digestion of proteins

About 1 mg of the desired protein (β-casein or α-casein) was dissolved in 1 mL of NH_4HCO_3 solution (25 mM, pH~8), and digested with trypsin at an enzyme-to-protein ratio of 1:40 (w/w) for 16 h at 37 °C. The digestion of BSA was performed by adding 20 μL of 100 mM DTT in 100 μL of 4 mg mL^{-1} BSA in 25 mM NH_4HCO_3 solution (pH~8) to incubate at 100 °C for 10 min, followed with cooling, addition of 20 μL of 1.0 M IAA, incubation in the dark for 45 min at room temperature, and addition of 20 μL of DTT to react with the excessive IAA at room temperature for 1 h, and finally 10-fold diluting the mixture with 25 mM NH_4HCO_3 and adding trypsin at an enzyme-to-protein ratio of 1:40 (w/w) to incubate for 16 h at 37 °C. For real samples, 30 μL of drinking milk was added in 900 μL of NH_4HCO_3 solution (25 mM, pH~8) and centrifugated at 16,000 rpm for 15 min to obtain the supernatant for tryptic digestion. After the supernatant was denaturated at 100 °C for 5 min, 30 μg of trypsin was added in the solution to digest at 37 °C for 16 h, which was then diluted 25 times with 0.5% TFA in 50% ACN (v/v). All the tryptic peptide mixtures were stored at −20 °C until use.

2.5. Selective enrichment of phosphopeptides

After the digestion product was further diluted with 0.5% TFA in 50% ACN (v/v), 50 μL of octahedral SnO_2 (6 mg mL^{-1}) was added into 200 μL of the diluted peptide mixture (Fig. 1). The mixture was then vibrated at 25 °C for 30 min and centrifuged to obtain the precipitates, which was washed thrice with 0.1% TFA in 60% ACN (v/v). The human serum sample could be directly used for phosphopeptide capture by mixing 30 μL sample with 120 μL of 0.5% TFA in 50% ACN (v/v) and then treating the mixture with octahedral SnO_2 (6 mg mL^{-1}). After the trapped phosphopeptide was eluted using 5 μL 10% $NH_3\cdot H_2O$ under sonication for 10 min, the eluate was analyzed by MALDI-TOF MS.

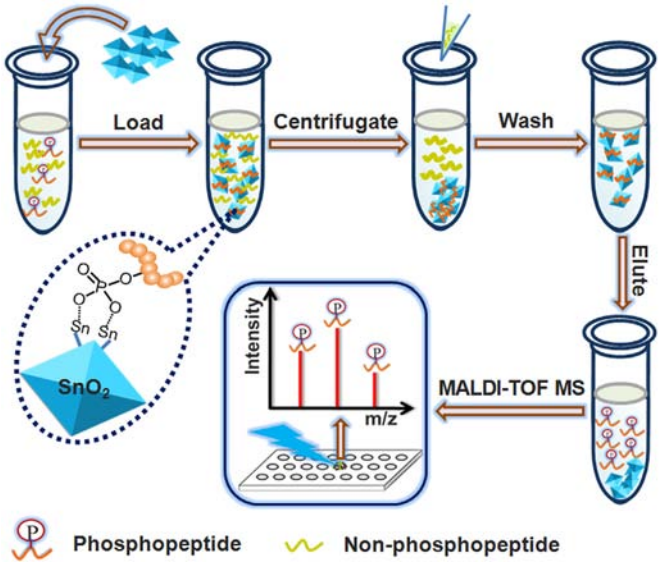

Fig. 1. Schematic illustration of selective enrichment of phosphopeptides using octahedral SnO_2 for mass spectrometric analysis.

2.6. MALDI-TOF MS analysis

After 0.5 μL of the eluate was deposited on a MALDI plate, 0.5 μL of 2, 5-DHB (20 mg mL^{-1}) in 50% ACN (v/v) containing 1% H_3PO_4 was introduced as a matrix to perform the MALDI-TOF MS analysis in a positive ion mode on a 4800 Proteomics Analyzer (Applied Biosystems, USA) with the Nd-YAG laser at 355 nm, a repetition rate of 200 Hz and an acceleration voltage of 20 kV.

3. Results and discussion

3.1. Preparation and characterization of octahedral SnO_2 nanoparticles

The crystalline structure of the as-prepared product was confirmed by X-ray diffraction (XRD). All the peaks in the XRD pattern could be indexed to the rutile phase of bulk SnO_2 with cell constants of $a=4.738$ and $c=3.187$ Å (JCPDS No. 41-1445) (Fig. 2a). The scanning electron microscopic (SEM) image of the SnO_2 nanoparticles showed a well-proportioned octahedral structure with a length of approximately 190 nm (Fig. 2b). Dynamic light scattering measurement also showed the hydrodynamic diameter of the SnO_2 nanoparticles to be about 200 nm with a narrow size distribution (Fig. S1, Supplementary material). More-detailed structural information of an individual octahedral SnO_2 particle was provided by transmission electron microscopy (TEM) (Fig. 2c). The corresponding selected-area electron diffraction (SAED) pattern could be indexed to the [$\bar{1}$10] zone axis of single-crystal tetragonal SnO_2 (inset in Fig. 2c). The apex angle between the two side surfaces was about 66.2°. These structural features agree well with the model of octahedral SnO_2 enclosed by {221} facets projected along the [$\bar{1}$10] direction [44]. The (221) surface can be described as combination of (111) terraces and (110) steps. Such a stepped surface composed of (111) terraces and (110) steps was directly captured in high-resolution TEM (Fig. 2d). These results clearly confirmed that the high-index facets {221} exposed octahedral SnO_2 nanoparticles were successfully obtained. And the synthesized material has abundant unsaturated coordination atoms, which usually exhibits high surface activity.

3.2. Selective enrichment of phosphopeptides from tryptic digestion of β-casein

In light of the unique characters of the synthesized octahedral SnO_2, its selective enrichment capacity toward phosphopeptides in the tryptic digest of bovine β-casein was firstly examined by MALDI-TOF MS. The direct analysis of β-casein digest without enrichment did not show the MS signals of the phosphopeptides due to the overwhelming of many dominant peaks of non-phosphopeptides in the sample (Fig. 3a). After selective enrichment by octahedral SnO_2, the signals of β1, β2 and β3 phosphopeptides could be observed (Fig. 3b). Moreover these peaks dominated the spectrum, indicating a good enrichment efficiency of the octahedral SnO_2. This result demonstrated the selectivity of octahedral SnO_2 nanoparticles toward phosphopeptides. The details of peptides detected in the MALDI-TOF spectra were summarized in Table S1 (Supplementary material).

To demonstrate the superiority of the high-index facets exposed octahedral SnO_2 for enrichment of phosphopeptides, SnO_2 nanosphere (Fig. S2, Supplementary material) and commercial TiO_2 were used for comparison. As shown in Fig. 3b–d, the mass spectrum using octahedral SnO_2 for enrichment exhibited three phosphopeptides with higher intensity than SnO_2 nanosphere and commercial TiO_2, indicating stronger capture ability. This was possibly due to the distinguished feature of octahedral SnO_2 with high densities of atom steps, ledges, kinks, and dangling bonds that usually exhibit high chemical-reaction activity. The β3 phosphopeptide exhibited more metastable losses of phosphoric acid (Fig. 3b) due to the high chemical-reaction activity of octahedral SnO_2 [37].

The detection limit of β-casein digest with enrichment by octahedral SnO_2 nanoparticles was also compared with that by SnO_2 nanosphere. In the digest of 4×10^{-9} M β-casein, the ion signals of β1, β2 and β3 phosphopeptides could still be detected after enrichment with octahedral SnO_2 nanoparticles (Fig. 4), while the MALDI mass spectrum after enrichment with SnO_2 nanosphere could not give clear signal of β3 phosphopeptide at the concentration of even 2×10^{-7} M, and the intensities for β1 and β2 at 4×10^{-9} M were lower than three times ratio of signal-to-noise (Fig. 5). The detection limit was comparable with

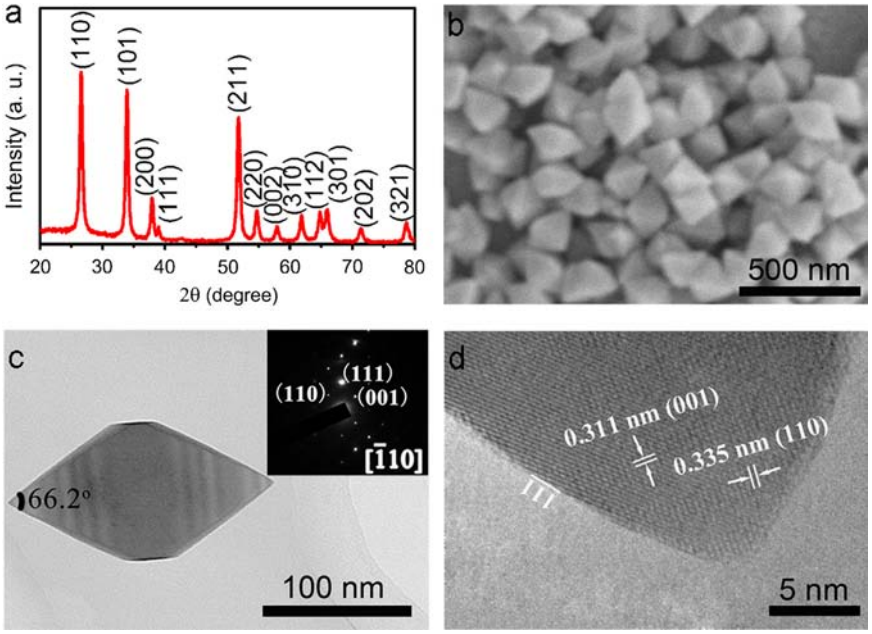

Fig. 2. (a) XRD pattern and (b) SEM image of octahedral SnO_2, (c) TEM image of single octahedral SnO_2 nanoparticle viewed along the [110] direction (inset: the corresponding SEAD pattern), and (d) high-resolution TEM image taken from the top apex of the octahedron.

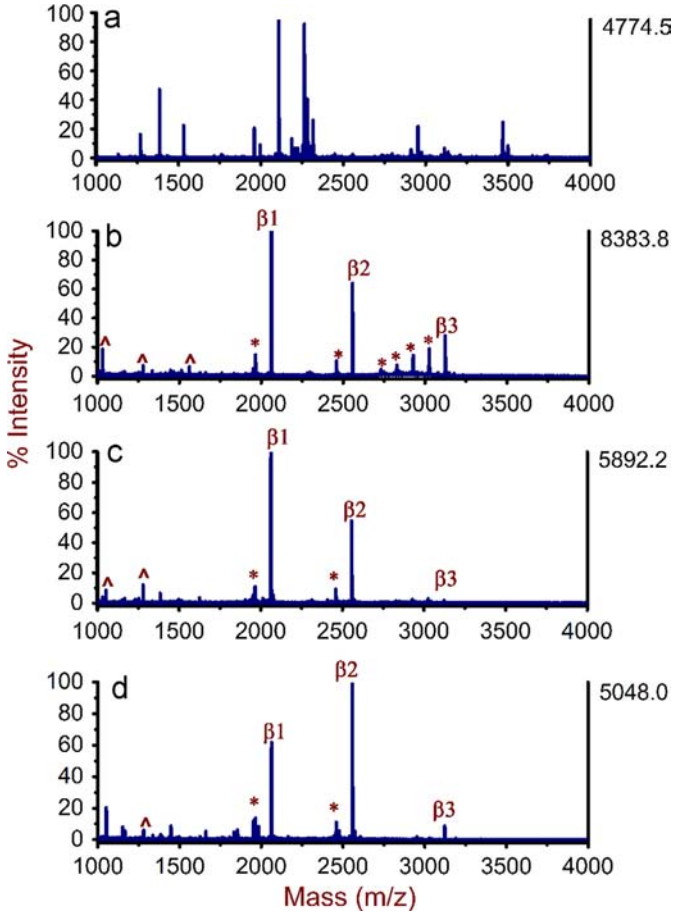

Fig. 3. MALDI mass spectra of tryptic digest of 4×10^{-8} M β-casein without (a) and with enrichment by octahedral SnO_2 nanoparticles (b), SnO_2 nanosphere (c) and commercial TiO_2 (d) (∗ metastable losses of phosphoric acid, ^ doubly charged phosphopeptide).

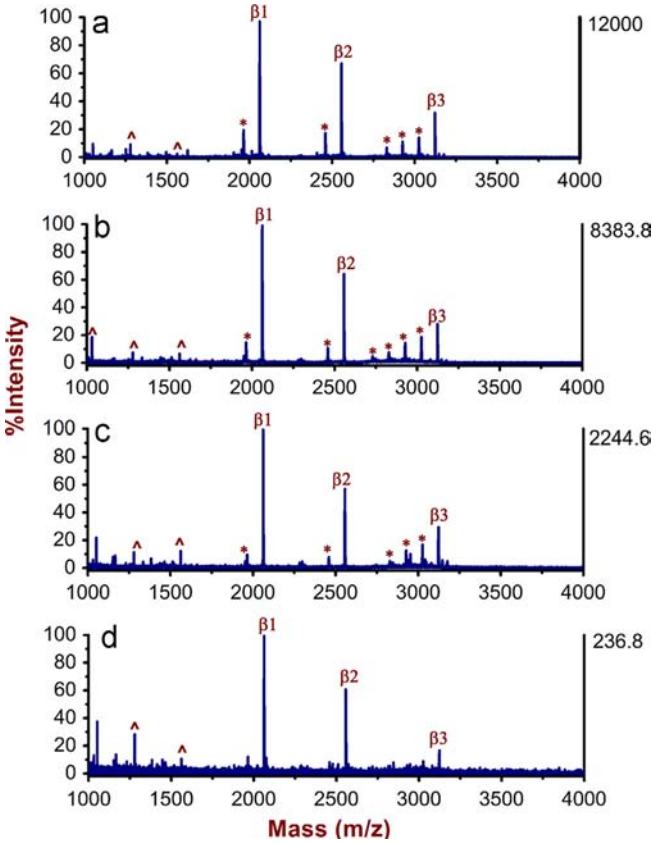

Fig. 4. MALDI mass spectra of tryptic digests of (a) 2×10^{-7}, (b) 4×10^{-8}, (c) 2×10^{-8} and (d) 4×10^{-9} M β-casein after enriched by octahedral SnO_2 nanoparticles (∗ metastable losses of phosphoric acid; ^ doubly charged phosphopeptide).

the previously reported Fe_3O_4@C@SnO_2 core–shell microspheres (2×10^{-9} M) [24] and α-Fe_2O_3@SnO_2 core–shell nanotubes (4×10^{-9} M) [25] for β-casein digest enrichment. The good sensitivity could be attributed to the abundant unsaturated coordination Sn atoms that exhibited enhanced affinity and selective coordination ability to phosphopeptides. The high detection sensitivity further suggested that the octahedral SnO_2 nanoparticles are promising nanomaterial for enrichment of phosphopeptides.

3.3. Highly specific enrichment of phosphorylated peptides from complex peptide mixtures

To further evaluate the enrichment specificity, a relatively complex sample, peptide mixture originating from a tryptic digest of β-casein and bovine serum albumin at molar ratio of 1:10 and 1:100, was used for test. Different from the direct analysis (Fig. 6a), the enrichment by octahedral SnO_2 excluded the interference with three phosphopeptides from the highly contaminated mixture, even at the BSA concentration 100 times higher than β-casein (Figs. 6b and 6c). The selectivity was much better than the previously reported Fe_3O_4@C@SnO_2 core–shell microspheres (1:50) [24] and α-Fe_2O_3@SnO_2 core–shell nanotubes (1:50) [25]. Furthermore, the high-concentration salt and denaturants such as ammonium bicarbonate, dithiothreitol and iodoacetamide used in the process of BSA digestion did not affect the specific capture of phosphopeptides. These results demonstrated the reliable performance of the octahedral SnO_2 nanoparticles in the selective capture of phosphopeptides from the complex peptide mixture.

3.4. Selective enrichment of phosphopeptides from tryptic digestion of α-casein

The selective capture ability of octahedral SnO_2 nanoparticles could be used for enrichment of more phosphopeptides. For example, in the absence of enrichment only two weak phosphopeptide peaks were observed for the tryptic digest of α-casein that contains more phosphopeptides, while the mass spectrum after enrichment showed 18 phosphopeptides with considerable intensities (Fig. 7). The detectable number exceeded those with Zr^{4+}–IMAC (14) [9] and Ti^{4+}–phosphate functionalized cellulose (14) [10] for α-casein digest enrichment. These results clearly indicated the high selectivity of the octahedral SnO_2 nanoparticles. The details of phosphopeptides detected in α-casein were listed in Table S2 (Supplementary material).

3.5. Highly specific enrichment of phosphopeptides from milk and human serum

Nonfat bovine milk contains two main phosphorylated proteins, α-casein and β-casein, which have been widely used as standard proteins for enrichment of phosphopeptides. The capability of octahedral SnO_2 to selectively trap phosphopeptides was thus evaluated using drinking milk as real samples. Fig. 8a displays the direct analysis of the tryptic digests of milk, in which non-phosphopeptides dominated the spectrum and only two weak peaks were generated from phosphopeptides. However, the mass

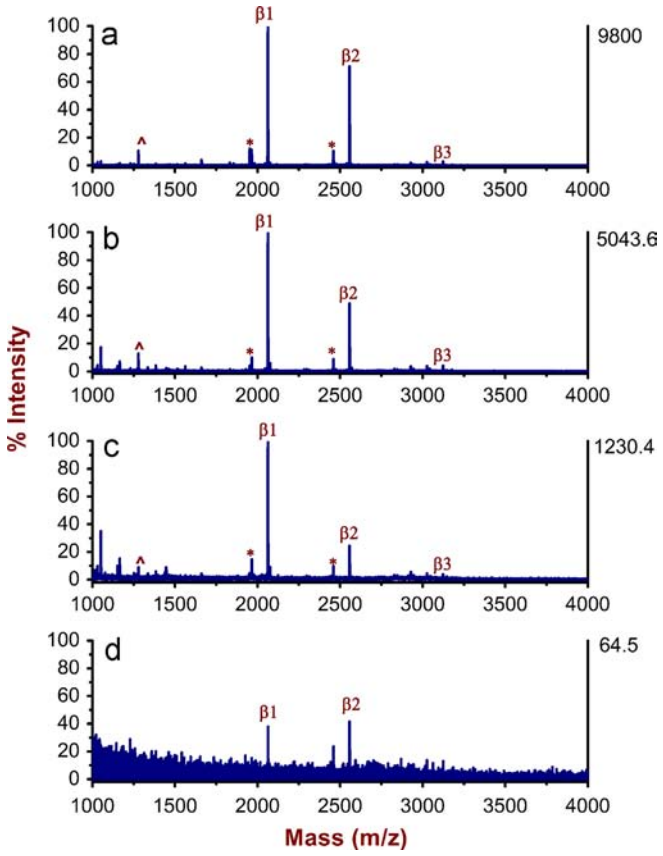

Fig. 5. MALDI mass spectra of tryptic digests of (A) 2×10^{-7}, (B) 4×10^{-8}, (C) 2×10^{-8} and (D) 4×10^{-9} M β-casein after enriched by SnO_2 nanosphere (* metastable losses of phosphoric acid; ^ doubly charged phosphopeptide).

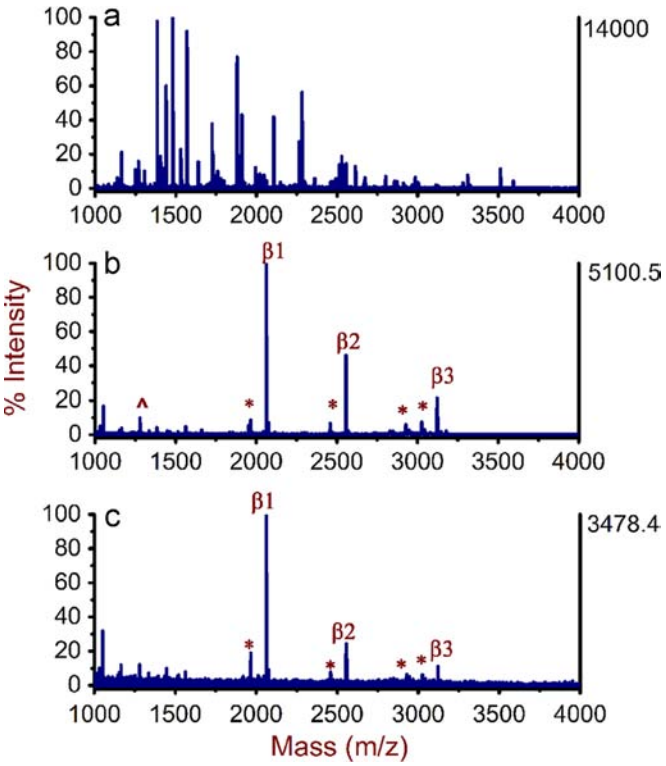

Fig. 6. MALDI mass spectra of tryptic digest of a mixture of β-casein/BSA at molar ratios of 1:10 for direct analysis (a) and with enrichment by octahedral SnO_2 (b), and (c) 1:100 with enrichment by octahedral SnO_2 (* metastable losses of phosphoric acid, ^ doubly charged phosphopeptide).

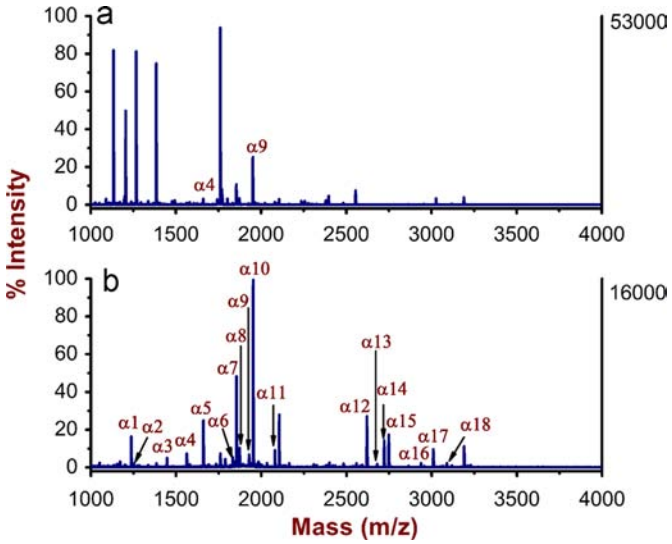

Fig. 7. MALDI mass spectra of tryptic digest of α-casein (a) without and (b) with enrichment by octahedral SnO_2 nanoparticles.

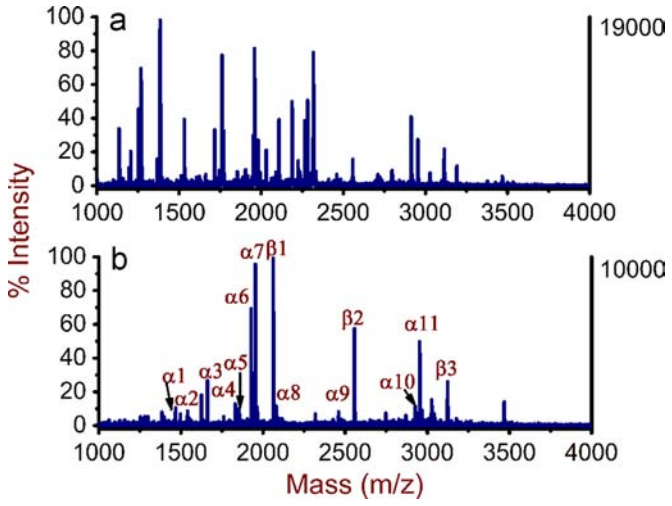

Fig. 8. MALDI mass spectra of tryptic digest of nonfat milk (a) without and (b) with enrichment by octahedral SnO_2.

spectrum of tryptic digest of nonfat milk was dominated by 14 phosphorylated peptide peaks after enrichment by octahedral SnO_2 (Fig. 8b, Table S3 in Supplementary material). It was much better than that with SnO_2 nanoparticles (10) and comparable with SnO_2–$ZnSn(OH)_6$ composite (15) [28]. The detectable number also exceeded the number using Ce^{4+}-chelated magnetic silica microspheres (10) [11]. Thus the octahedral SnO_2 nanoparticles possessed high selectivity and effectiveness in enrichment of phosphopeptides from real biological samples.

The human serum sample was also used for testing the specificity in enrichment of endogenous low-abundant phosphopeptides. The direct analysis of human serum is not shown here due to the presence of extremely high concentrations of salts that led to significant suppression of ionization in MALDI. Human serum sample without digestion showed four peaks of phosphopeptides derived from phosphorylated fibrinopeptide A [45], and some phosphopeptides showed the metastable losses of phosphoric acid (Fig. 9 and Table S4, Supplementary material). These results support the capability of octahedral SnO_2 to selectively isolate and enrich phosphopeptides from the extremely complicated biological system.

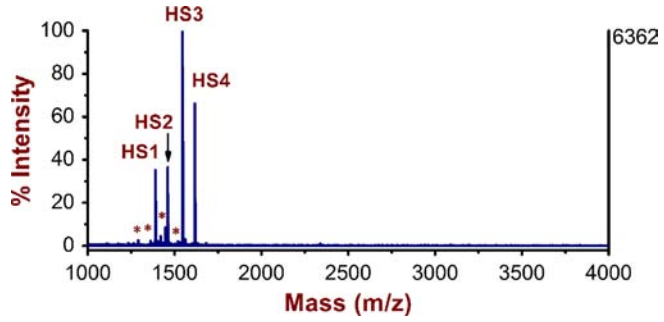

Fig. 9. MALDI mass spectrum of human serum sample after enriched by octahedral SnO_2 nanoparticles (* metastable losses of phosphoric acids).

4. Conclusions

Octahedral SnO_2 nanoparticles with exposed high-energy {221} facets were firstly applied in the selective capture and enrichment of phosphopeptides. The octahedral SnO_2 showed strong affinity to phosphopeptides by forming the bidentate bonds between high-density surface atoms and phosphate, and thus can achieve the selective enrichment of phosphopeptides. The octahedral SnO_2 shows excellent performance for selective enrichment of phosphopeptides from real complex samples. The advantages of this material for enrichment include its high adsorption capacity, high selectivity, easy separation from solution, and high sensitivity for mass spectroscopic detection. All the tests indicated that the octahedral SnO_2 can act as an ideal adsorbent for phosphopeptides. This work provides a way to improve the physical and chemical properties of materials for selective enrichment of phosphopeptides, and extends the application of metal oxides with high-energy facets in molecular identification, especially in the MS-based phosphoproteomic study.

Acknowledgments

This work was financially supported by the National Basic Research Program of China (2010CB732400), National Natural Science Foundation of China (21121091 and 21135002).

Appendix A. Supplementary material

Supplementary data associated with this article can be found in the online version at http://dx.doi.org/10.1016/j.talanta.2013.11.049.

References

[1] T. Hunter, Cell 100 (2000) 113–127.
[2] J. Ptacek, G. Devgan, G. Michaud, H. Zhu, X.W. Zhu, J. Fasolo, H. Guo, G. Jona, A. Breitkreutz, R. Sopko, R.R. McCartney, M.C. Schmidt, N. Rachidi, S.J. Lee, A.S. Mah, L.H. Meng, M.J.R. Stark, D.F. Stern, C.D. Virgilio, M. Tyers, B. Andrews, M. Gerstein, B. Schweitzer, P.F. Predki, M. Snyder, Nature 438 (2005) 679–684.
[3] M. Bollen, M. Beullens, Trends Cell Biol. 12 (2002) 138–145.
[4] J.V. Olsen, B. Blagoev, F. Gnad, B. Macek, C. Kumar, P. Mortensen, M. Mann, Cell 127 (2006) 635–648.
[5] R. Aebersold, M. Mann, Nature 422 (2003) 198–207.
[6] H.L. Zhou, J.D. Watts, R. Aebersold, Nat. Biotechnol. 19 (2001) 375–378.
[7] L. Andersson, J. Porath, Anal. Biochem. 154 (1986) 250–254.
[8] J.Y. Ye, X.M. Zhang, C. Young, X.L. Zhao, Q. Hao, L. Cheng, O.N. Jensen, J. Proteome Res. 9 (2010) 3561–3573.
[9] H. Wang, J.C. Duan, H.J. Xu, L. Zhao, Y. Liang, Y.C. Shan, L.H. Zhang, Z. Liang, Y.K. Zhang, J. Sep. Sci. 34 (2011) 2113–2121.
[10] F. Shen, Y.F. Hu, P. Guan, X.Q. Ren, J. Chromatogr. B 902 (2012) 108–115.
[11] Y. Li, D.W. Qi, C.H. Deng, P.Y. Yang, X.M. Zhang, J. Proteome Res. 7 (2008) 1767–1777.
[12] J. Rush, A. Moritz, K.A. Lee, A. Guo, V.L. Goss, E.J. Spek, H. Zhang, X.M. Zha, R.D. Polakiewicz, M.J. Comb, Nat. Biotechnol. 23 (2005) 94–101.
[13] G.A. Zhang, T.A. Neubert, Proteomics 6 (2006) 571–578.
[14] A. Leitner, Trends Anal. Chem. 29 (2010) 177–185.
[15] M.R. Larsen, T.E. Thingholm, O.N. Jensen, P. Roepstorff, T.J.D. Jørgensen, Mol. Cell. Proteomics 4 (2005) 873–886.
[16] F. Wolschin, S. Wienkoop, W. Weckwerth, Proteomics 5 (2005) 4389–4397.
[17] N. Sugiyama, T. Masuda, K. Shinoda, A. Nakamura, M. Tomita, Y. Ishihama, Mol. Cell. Proteomics 6 (2007) 1103–1109.
[18] H.K. Kweon, K. Håkansson, Anal. Chem. 78 (2006) 1743–1749.
[19] W.F. Ma, Y. Zhang, L.L. Li, L.J. You, P. Zhang, Y.T. Zhang, J.M. Li, M. Yu, J. Guo, H.J. Lu, C.C. Wang, ACS Nano 6 (2012) 3179–3188.
[20] J. Lu, M.Y. Wang, C.H. Deng, X.M. Zhang, Talanta 105 (2013) 20–27.
[21] H.Y. Bi, L. Qiao, J.M. Busnel, V. Devaud, B.H. Liu, H.H. Girault, Anal. Chem. 81 (2009) 1177–1183.
[22] J. Lu, S.S. Liu, C.H. Deng, Chem. Commun. 47 (2011) 5334–5336.
[23] M. Sturm, A. Leitner, J.H. Smått, M. Lindén, W. Lindner, Adv. Funct. Mater. 18 (2008) 2381–2389.
[24] D.W. Qi, J. Lu, C.H. Deng, X.M. Zhang, J. Phys. Chem. C 113 (2009) 15854–15861.
[25] J. Lu, D.W. Qi, C.H. Deng, X.M. Zhang, P.Y. Yang, Nanoscale 2 (2010) 1892–1900.
[26] A. Leitner, M. Sturm, J.H. Smått, M. Järn, M. Lindén, K. Mechtler, W. Lindner, Anal. Chim. Acta 638 (2009) 51–57.
[27] A. Leitner, M. Sturm, O. Hudecz, M. Mazanek, J.H. Smått, M. Lindén, W. Lindner, K. Mechtler, Anal. Chem. 82 (2010) 2726–2733.
[28] L.P. Li, T. Zheng, L.N. Xu, Z. Li, L.D. Sun, Z.X. Nie, Y. Bai, H.W. Liu, Chem. Commun. 49 (2013) 1762–1764.
[29] G.Z. Fang, W. Gao, Q.L. Deng, K. Qian, H.T. Han, S. Wang, Anal. Biochem. 423 (2012) 210–217.
[30] H.Y. Zhong, X. Xiao, S. Zheng, W.Y. Zhang, M.J. Ding, H.Y Jiang, L.L. Huang, J. Kang, Nat. Commun. 4 (2013) p1656.
[31] L. Zhao, R.A. Wu, H.F. Zou, Methods Mol. Biol. 790 (2011) 215–222.
[32] P.X. Zhao, Y Zhao, X.F Guo, H. Wang, H.S. Zhang, J. Chromatogr. A 1218 (2011) 2528–2539.
[33] Q. Kuang, C.S. Lao, Z. Li, Y.Z. Liu, Z.X. Xie, L.S. Zheng, Z.L. Wang, J. Phys. Chem. C 112 (2008) 11539–11544.
[34] Y.T. Wan, J.Y. Liu, X.Q. Fu, X.M. Zhang, F.L. Meng, X.Y. Yu, Z. Jin, L.T. Kong, J.H. Liu, Talanta 99 (2012) 394–403.
[35] S. Gubbala, V. Chakrapani, V. Kumar, M.K. Sunkara, Adv. Funct. Mater. 18 (2008) 2411–2418.
[36] M.S. Park, G.X. Wang, Y.M. Kang, D. Wexler, S.X. Dou, H.K. Liu, Angew. Chem., Int. Ed. 46 (2007) 750–753.
[37] N. Tian, Z.Y. Zhou, S.G. Sun, Y. Ding, Z.L. Wang, Science 316 (2007) 732–735.
[38] D.B. Fan, P.J. Thomas, P.O. Brien, J. Am. Chem. Soc. 130 (2008) 10892–10894.
[39] H.G. Liao, Y.X. Jiang, Z.Y. Zhou, S.P. Chen, S.G. Sun, Angew. Chem., Int. Ed. 47 (2008) 9100–9103.
[40] M. Leng, M.Z. Liu, Y.B. Zhang, Z.Q. Wang, C. Yu, X.G. Yang, H.J. Zhang, C. Wang, J. Am. Chem. Soc. 132 (2010) 17084–17087.
[41] H.G. Yang, C.H. Sun, S.Z. Qiao, J. Zou, G. Liu, S.C. Smith, H.M. Cheng, G.Q. Lu, Nature 453 (2008) 638–642.
[42] X.W. Xie, Y. Li, Z.Q. Liu, Q. Haruta, W.J. Shen, Nature 458 (2009) 746–749.
[43] Y.Y. Ma, Q. Kuang, Z.Y. Jiang, Z.X. Xie, R.B. Huang, L.S. Zheng, Angew. Chem., Int. Ed. 47 (2008) 8901–8904.
[44] X.G. Han, M.S. Jin, S.F. Xie, Q. Kuang, Z.Y. Jiang, Y.Q. Jiang, Z.X. Xie, L.S. Zheng, Angew. Chem., Int. Ed. 48 (2009) 9180–9183.
[45] H.Y. Lin, W.Y. Chen, Y.C. Chen, Anal. Bioanal. Chem. 394 (2009) 2129–2136.